Fiducial Reference Measurements for Ground-Based DOAS Air-Quality Observations

ESA Contract No. 4000135355/21/I-DT-lr

Deliverable D8.1:

Technical note on BrO Slant Column Fitting Optimisation

Date: 14/10/2025

Version: 1.1

Contributing authors:

Michel Van Roozendael, Martina M. Friedrich, Alexis Merlaud, Gaia Pinardi (BIRA-IASB)

Rob Ryan (University of Melbourne (UOM/ ABOM)

Thomas Wagner (MPIC)

Udo Friess (IUPHD)

Andreas Richter (IUP-UB)

Alexander Cede, Martin Tiefengraber (Luftblick)

Mark Wenig (LMU)

Kim Strong, Ramina Alwarda, Darby Bates (UoT)

Hyeong-Ahn Kwon, Jong-Uk Park (SUWON)

Ang Li, Pinhua Xie, Yuhan Luo, Chaonan Lv, Zhaokun Hu (AIOFM)

Dimitris Karagkiozidis, Dimitris Nikolis (AUTH)

Elisa Castelli, Andrè Achilli (CNR-ISAC)

Ka Lok Chan (RAL)

Ankie Piters (KNMI)

Cheng Liu, Xing Chengzhi (USTC)

Richard Querel (NIWA)

Cristina Prados-Roman, Mónica Navarro-Comas, Margarita Yela (INTA)

Table of Contents

List of acronyms

AIOFM	Anhui Institute of Optics and Fine Mechanics, Hefei, China
AIRYX	Airyx GmbH
ABOM	Australian Bureau of Meteorology, Melbourne, Australia
AUTH	Laboratory of Atmospheric Physics, Aristotle University of Thessaloniki, Thessaloniki, Greece
BIRA-IASB	Royal Belgian Institute for Space Aeronomy (BIRA-IASB), Brussels, Belgium
CINDI-3	Third Cabauw Intercomparison of UV-Vis DOAS Instruments
CNR-ISAC	Consiglio Nazionale delle Ricerche - Istituto di Scienze dell'Atmosfera e del Clima, Bologna, Italy
DOAS	Differential Optical Absorption Spectroscopy
ESA	European Space Agency
FOV	Field of View
FRM4DOAS	Fiducial Reference Measurements for Ground-Based DOAS Air-Quality Observations
FWHM	Full Width at Half Maximum
INTA	Instituto Nacional de Técnica Aeroespacial, Madrid, Spain
CNR-ISAC	Institute of Atmospheric Sciences and Climate, Bologna, Italy
ISRF	Instrumental Spectral Response Function
IUP-UB	Institute of Environmental Physics (IUP), University of Bremen, Bremen, Germany
IUPH	Institute of Environmental Physics, Heidelberg University
KNMI	Royal Netherlands Meteorological Institute, De Bilt, The Netherlands
LATMOS	Laboratoire Atmosphère, Milieux, Observations Spatiales, Guyancourt, France
LBLICK	Luftblick OG
LMU	Ludwig Maximilian University of Munich, Germany
MAX-DOAS	Multi-Axis DOAS
MPIC	Max Planck Institute for Chemistry, Mainz, Germany
NDACC	Network for the Detection of Atmospheric Composition Changes
NIWA	National Institute of Water and Atmospheric Research
PGN	Pandonia Global Network
PKNU	Pukyong National University, Busan, South Korea
UOM	University of Melbourne, Australia
RAL	Rutherford Appleton Laboratory Space, UK
SUWON	University of Suwon, Hwaseong-si, Republic of Korea
UOT	Department of Physics, University of Toronto, Toronto, Canada
USTC	University of Science and Technology of China, Hefei, China

1. Introduction

Although stratospheric BrO columns have been monitored for more than two decades, the availability of such measurements remains limited to a few sites worldwide and the continuity of the time series is not guaranteed due to a lack of operationalization of the processing chains. Motivated by the need to gather suitable BrO validation data set for the upcoming ALTIUS satellite mission, ESA recently decided to support the development of an operational BrO processing chain as part of the FRM4DOAS data processing system. In its current state, FRM4DOAS includes processors for NO_2, O_3, H_2CO and aerosol retrievals. Stratospheric NO_2 retrievals are based on zenith-sky twilight measurements and use an optical estimation approach for the inversion of vertical concentration profiles with maximum information content between 10 and 35 km of altitude. Using a similar retrieval approach, stratospheric BrO vertical profile information can be derived from zenith-sky measurements in the wavelength range 346-360 nm (Hendrick et al., 2007). The aim is to integrate and adapt existing tools and enable their application at FRM4DOAS sites equipped with suitable instruments, i.e. spectrometers covering the UV spectral range with enough sensitivity to allow for good quality BrO slant column measurements during twilight conditions (typically between 80 and 90 deg of solar zenith angle).

One of the reasons explaining the current sparsity of BrO data is that analysis for BrO using the differential optical absorption spectroscopy (DOAS) technique has always been challenging, leading to uncertainty about the accuracy of measurements. Although this issue has already been addressed in previous studies (e.g. Aliwell et al., 2002), the availability of new spectroscopic data and the development of improved methods to deal with the typically strong ozone absorption at twilight are a motivation to revisit the BrO retrieval settings. This is the purpose of the work developed in this report, which starts with the exploitation of measurements performed during the Third Cabauw Intercomparison of UV-Vis DOAS Instruments (CINDI-3).

2. Overview of BrO measurements submitted during the CINDI-3 campaign

22 groups submitted BrO differential slant column density (dSCD) data based on instruments listed in Table 1. A subset of the participating groups also joined the on-site FRM4DOAS central processing exercise organized by BIRA and submitted L1 (spectra) files in a common data format. The corresponding instruments, which are used later in this report, are highlighted in green in Table 1.

The BrO spectral analysis was performed by individual teams using common retrieval settings defined for the campaign as described in Table 2. These settings are strongly inspired by the settings recommended in the Aliwell et al. (2002) paper, with minor updates as to the laboratory cross-sections used but based on the same spectral interval for the DOAS fit (346-359 nm). Reference spectra were obtained from noon-time zenith measurements averaged during a 10’ interval between 11:35 and 11:45 UTC. Although BrO retrievals were also performed using a fixed reference spectrum, we limit the present analysis to daily reference data.

Table 1: Characteristics of the instruments having reported BrO slant column data during the CINDI-3 campaign. The instruments highlighted in green also participated to the FRM4DOAS exercise, and therefore also submitted L1 data in a common data format.

#	Institute acronym	Instrument PI	Instrument type	Spectral range (UV channel)	ISRF FWHM (nm)	Det. Temp (°C)
01	ABOM	Rob Ryan	SkySpec-1D	296-460 nm	0.6	20
02	UOM	Rob Ryan	SkySpec-1D	296-410 nm	0.6	20
05	MPIC	Thomas Wagner	Tube-DOAS	300-460 nm	0.65	20
06	UOT	Kim Strong	SkySpec-1D	300-540 nm	0.6	20
07	SUWON	Hyeong-Ahn Kwon	SkySpec-1D	300-460 nm	< 0.7	20
14	LMU	Mark Wenig	SkySpec-1D	300-460 nm	0.6	20
15	AIOFM	Ang Li	2D-MAXDOAS	290-450 nm	0.4	25
16	AIOFM	Pinhua Xie	2D-MAXDOAS	220-430 nm	0.35	-40
17	AIOFM	Yuhan Luo	2D-MAXDOAS	290-420 nm	0.55	25
19	AUTH	Dimitris Karagkiozidis	DELTA	305-523 nm	0.85	-50
20	BIRA	Michel Van Roozendael	2D-MAXDOAS	304-383 nm	0.35	-50
21	BIRA	Alexis Merlaud	SkySpec-2D	297-462 nm	0.55	10
24	CNR-ISAC	Elisa Castelli	SkySpec-2D	300-405 nm	0.45	20
25	IUP-UB	Kai Krause	2D-MAXDOAS	315-376 nm	0.21	-45
28	IUPHD	Udo Frieß	SkySpec-2D	300-550 nm	0.6	20
29	IUPH	Udo Frieß	PMAX-DOAS	285-565 nm	1.3	-28
33	RAL	Ka Lok Chan	SkySpec-2D	310-410 nm	0.45	20
34	KNMI	Ankie Piters	Pandora-1S	280-530 nm	0.6	25-26
35	LBLICK	Martin Tiefengraber	Pandora-1S	280-530 nm	0.6	25-26
36	LBLICK	Martin Tiefengraber	Pandora-1S	280-530 nm	0.6	25-26
39	USTC	Cheng Liu	SkySpec-2D	297-409 nm	0.45	20

Table 2: BrO slant column retrieval settings specified for use during the CINDI-3 campaign.

Wavelength range	346.0-359.0 nm
Fraunhofer reference spectra	MAX-DOAS: daily noon reference spectrum (11:35 - 11:45 UTC)
Cross-sections:	
BrO (223 K)	Fleischmann et al. (2004)
NO_2 (220 K)	Vandaele et al. (1998) with I_0 correction (SCD of 10^{17} molec/cm^2)
O_3 (223 K)	Serdyuchenko et al. (2014) with I_0 correction (SCD of 10^{20} molec/cm^2) and Taylor terms (Pukite et al., 2010)
O_3 (243 K)	Serdyuchenko et al. (2014) with I_0 correction (SCD of 10^{20} molec/cm^2), orthogonalized to O_3 (223K)

O_4 (293 K)	Finkenzeller et al. (2022)
Ring	Normalised Ring spectrum based on Wagner et al. (2009) and slope term
Polynomial degree	Order 2 (3 coefficients)
Intensity offset	Slope (order 1)
Shift and stretch	Each measured spectrum is aligned on the reference using shift and stretch

Figure 1 shows an example of spectral retrieval obtained using standard settings, based on the BIRA-IASB instrument (#20). In this spectral range, two prominent absorption bands of BrO are included. The main interfering features are due to ozone absorption and the Ring effect, but in this spectral range, ozone remains a moderate absorber.

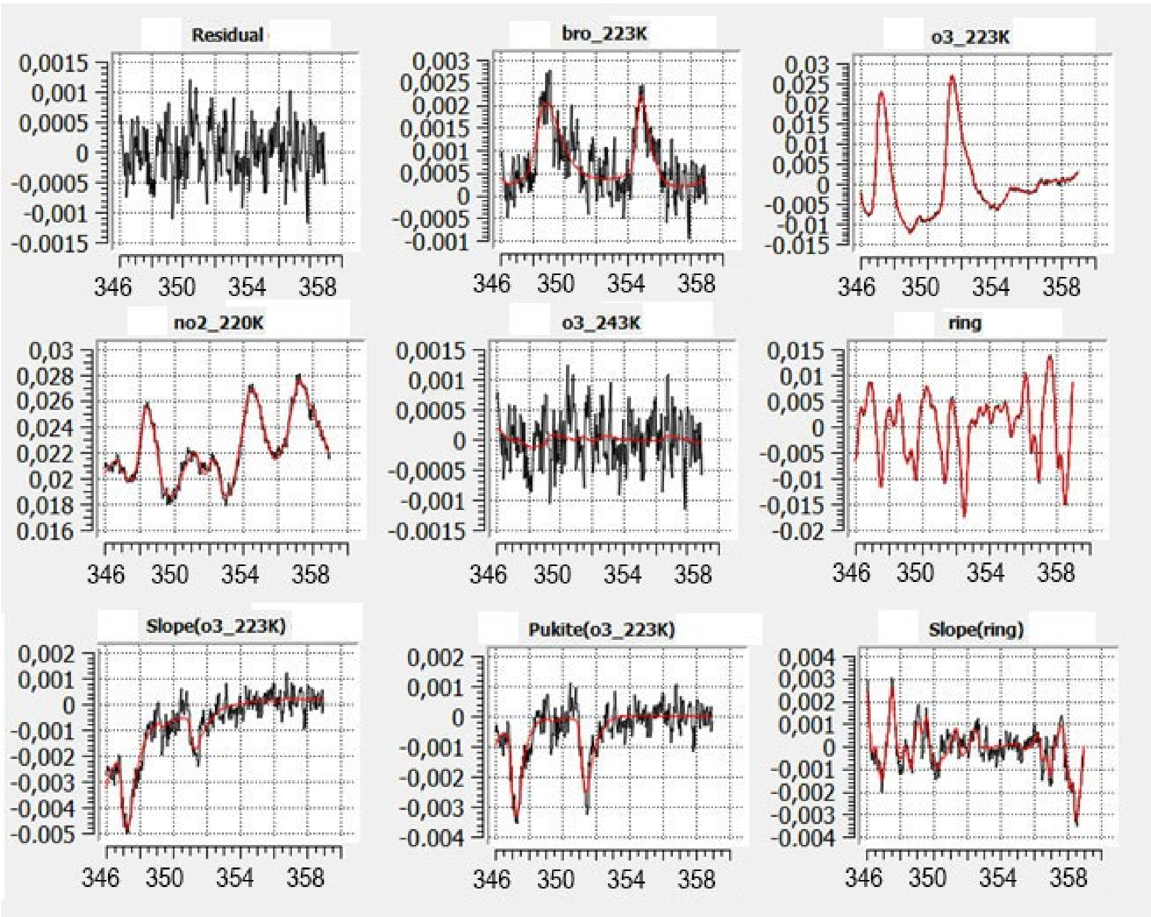

Figure 1: Example of BrO fit retrieval obtained using spectra from instrument #20 (BIRA-IASB) and analysis settings described in Table 2. Results correspond to measurements performed on 02/06/2024 at 90° SZA, morning. The reference spectrum was selected at noon, on the same day.

Figure 2 displays the BrO dSCDs retrieved from all participating instruments on 14 June 2025, evening. We only considered the most recent version from each dataset, indicated in the legend of the figure, next to the instrument's name. As can be seen, the scatter of the data is high indicating that some instruments struggle to detect BrO. The black thick line denotes the median value calculated from all instruments, in bins of 1 degree of solar zenith angle. We consider these medians as the most probable approximation of the true BrO dSCD values. The same procedure was applied to all measurement days, and separately for morning and evening data. This forms an ensemble of reference values suitable for comparison with individual datasets.

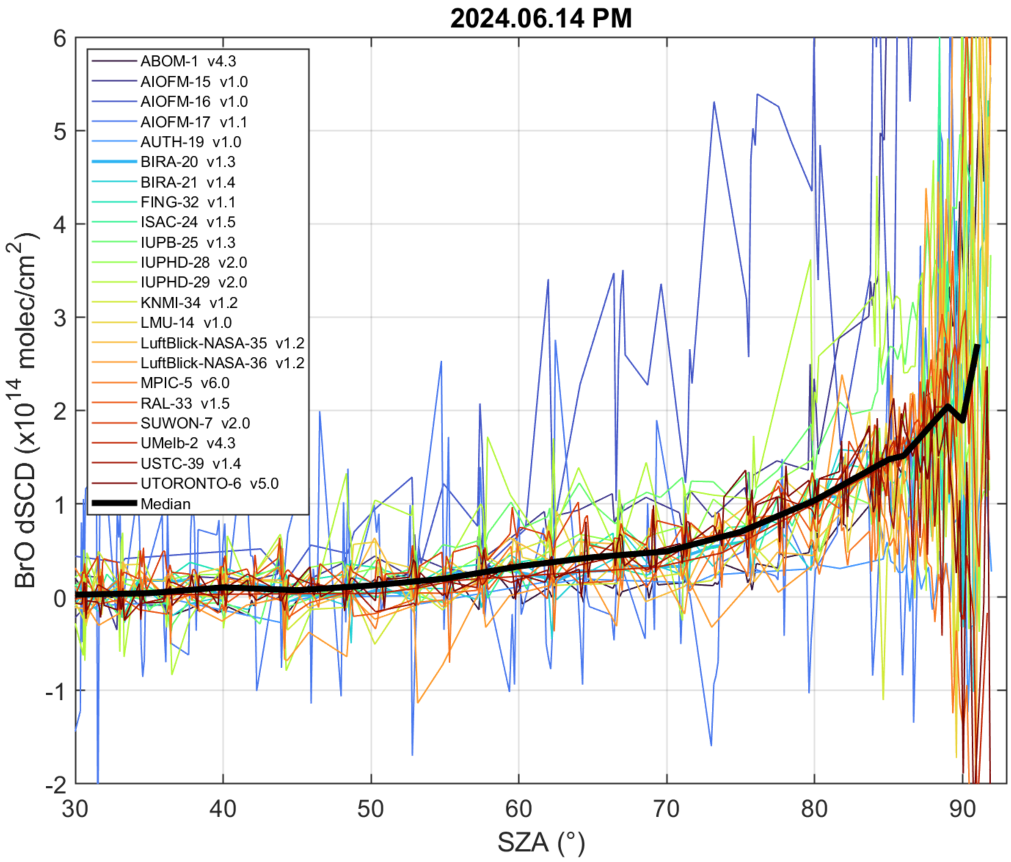

Figure 2: BrO differential slant columns retrieved from all participants in the evening of 14 June 2025. The thick black curve denotes the median values, calculated from all data in bins of 1 degree SZA.

Using median dSCD values as reference, linear regression plots were generated for each instrument, considering the complete measurement period. Results from this analysis are displayed in Figure 3. For each comparison case, the Pearson regression coefficient and the RMS from the regression fit are indicated. It is clear from the figure that the level of consistency with the medians differs quite a lot depending on the instrument considered. Some instruments show a compact relationship, while others deviate more strongly. In some cases, the noise level is extremely large, indicating a lack of sensitivity for BrO retrieval.

3. Extended BrO retrieval settings

We tested several alternative recovery options with the aim of improving the spectral information content by broadening the wavelength range of the fitting interval. Tests were performed using 2, 3 and 4 bands of BrO . The difficulty lies in managing the higher absorption of ozone, which develops at shorter UV wavelengths and generally causes spectral interference that biases BrO recovery. To minimize these effects, we tested the benefit of including additional ozone-related correction terms, namely (1) the so-called Pukite terms (Pukite at al., 2010) that account for deviations to the DOAS approximation under strong absorption conditions, and (2) the explicit treatment of the impact of ozone absorption on the Ring effect (the so-called molecular Ring effect, see Lerot et al., 2014).

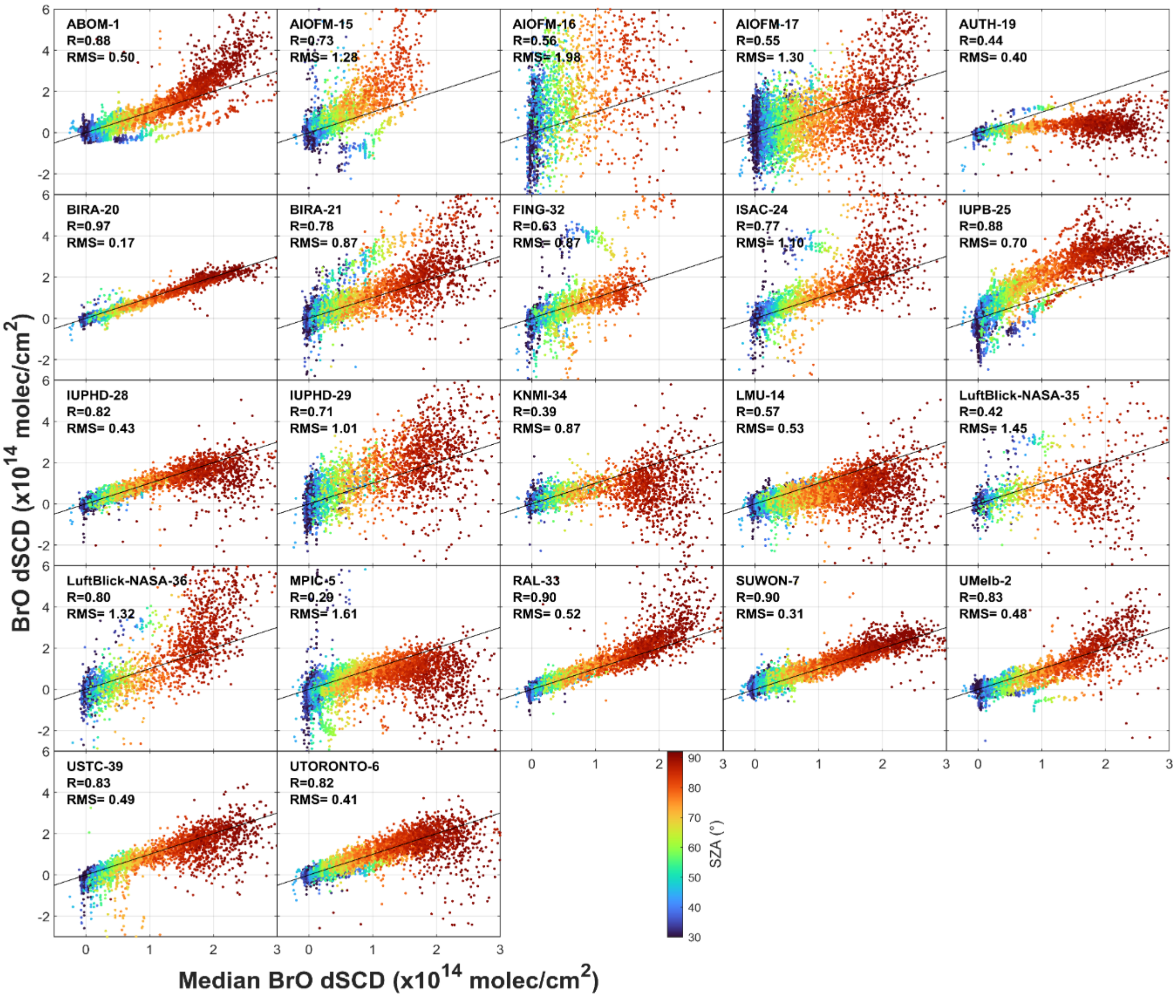

Figure 3: Linear correlation plots between individual BrO dSCD datasets and median values calculated as shown in Figure 2. Values are color coded according to the solar zenith angle. The statistical parameters (Person correlation coefficient and RMS from the linear regression fit) are given in the insert.

The proposed extended retrieval settings are summarised in Table 3. They use a fitting interval from 336.5 to 359 nm that covers 4 bands of BrO absorption. In addition, HCHO is explicitly included in the fit and a second Ring cross-section calculated at 220 K is added to account for the temperature dependence of the Ring effect.

Table 3: Slant column retrieval settings optimised for BrO retrieval using 4 absorption bands.

Wavelength range	336.5-359.0 nm
Fraunhofer reference spectra	MAX-DOAS: daily noon reference spectrum (11:35 - 11:45 UTC)
Cross-sections:	
BrO (223 K)	Fleischmann et al. (2004)
NO_2 (220 K)	Vandaele et al. (1998) with I_0 correction (SCD of 10^{17} molec/cm^2)
HCHO (298 K)	Meller and Moortgat (2000)
O_3 (223 K)	Serdyuchenko et al. (2014) with I_0 correction (SCD of 10^{20} molec/cm^2) and Taylor terms (Pukite et al., 2010)

O_3 (243 K)	Serdyuchenko et al. (2014) with I_0 correction (SCD of 10^{20} molec/cm^2), orthogonalized to O_3 (223K)
O_4 (293 K)	Finkenzeller et al. (2022)
Ring (250 K)	Normalised Ring spectrum based on Wagner et al. (2009) + slope term + molecular correction for O_3 absorption (223 K)
Ring (220 K)	Second Ring cross-section calculated at 220°K and orthogonalized to Ring (250 K)
Polynomial degree	Order 5 (6 coefficients)
Intensity offset	Slope (order 1)
Shift and stretch	Each measured spectrum is aligned on the reference using shift and stretch

Figure 4 shows an example of spectral retrieval obtained using the new settings. Measurement conditions are similar to those selected for Figure 1 (twilight data at 90° SZA), however they are not identical. The strength of the ozone absorption is clearly apparent (more than an order of magnitude larger than in the 346-359 nm interval) and justifies the need to apply the Pukite correction terms. These corrections are essential to obtain satisfying BrO fitting results.

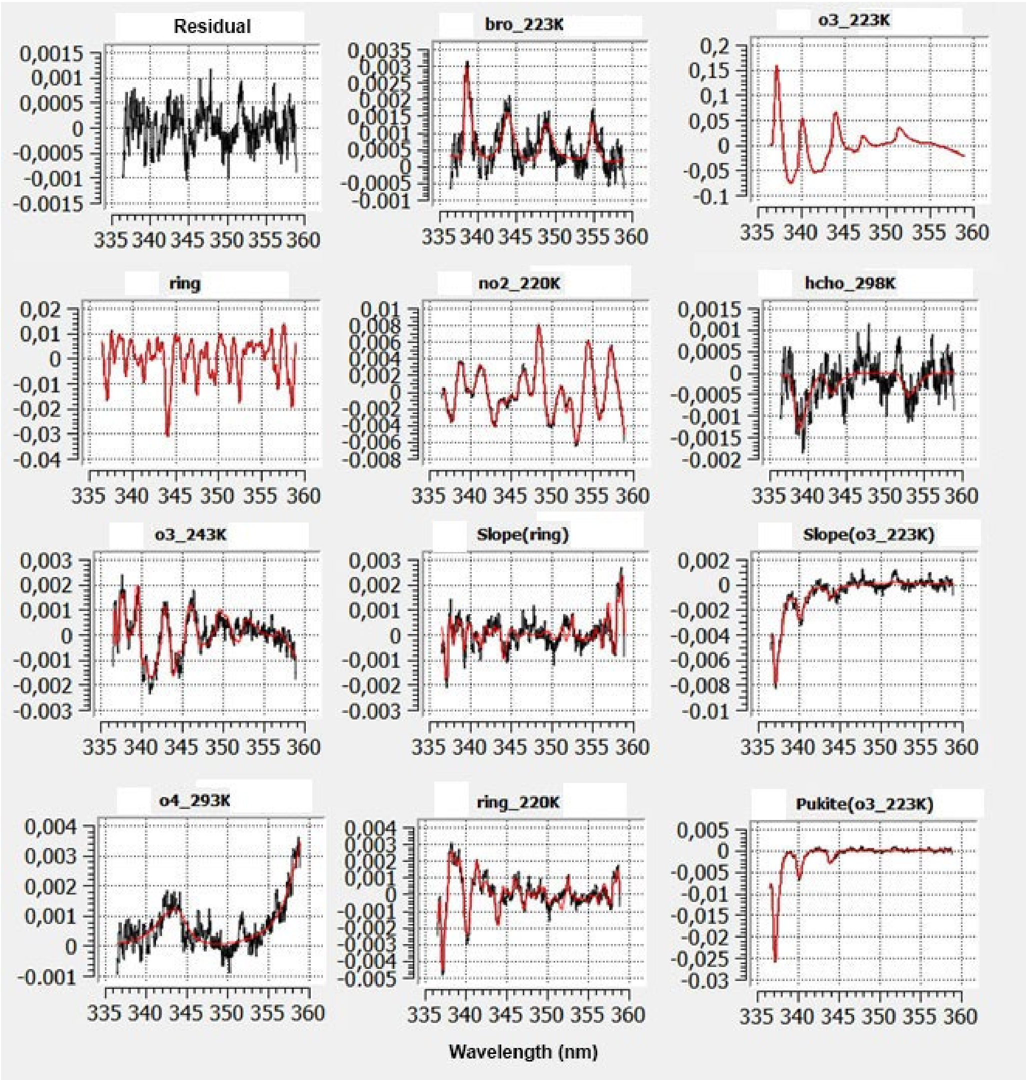

Figure 4: Example of BrO spectral fit using the extended analysis settings described in Table 3. Results correspond to measurements performed using instrument #20 on 06/06/2024 at 90° SZA, evening. The reference spectrum was selected at noon, on the same day.

We have applied the new settings to data from instrument #20 and compared the resulting BrO dSCDs on the different days of the campaign. Results are displayed in Figures 5 (a) and 5 (b) respectively. As can be seen, the new settings result in significantly smoother BrO dSCDs, especially for off-axis measurements. Roughly speaking, the mean level of agreement between both evaluations appears to be good, although the 4-band analysis seems to produce slightly smaller values at large SZA. This feature will be further discussed later.

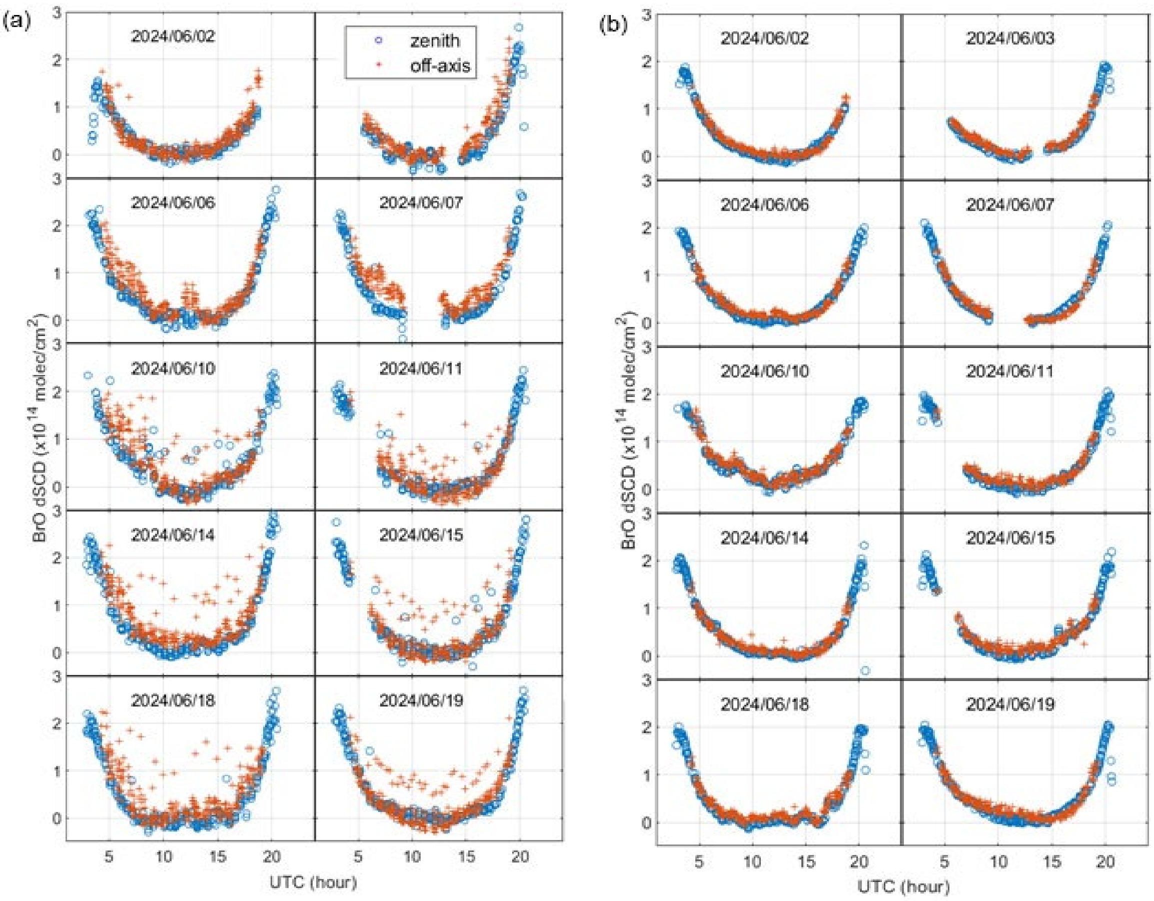

Figure 5: Time-series of BrO dSCDs retrieved from instrument #20 using standard fit settings (a) and extended settings (b). The benefit of the new settings in terms of noise reduction is obvious, especially on off-axis data.

4. Application of the extended settings to CINDI-3 measurements

To test the applicability of the new settings to more instruments, we exploited the L1 data from the teams having participated to the FRM4DOAS central processing exercise (see Table 1). These data use a common netCDF data format compatible with the QDOAS software, which makes their integration easy. QDOAS configuration templates were generated in a consistent way for all instruments, so that a central processing of the BrO dSCD could be performed. To test the system, we first run the evaluation using the standard campaign settings. Results are displayed in Figure 5 and show similar patterns to those obtained using individually processed data (see Figure 3). Note that, for a fair comparison, the same median values were used in both analysis.

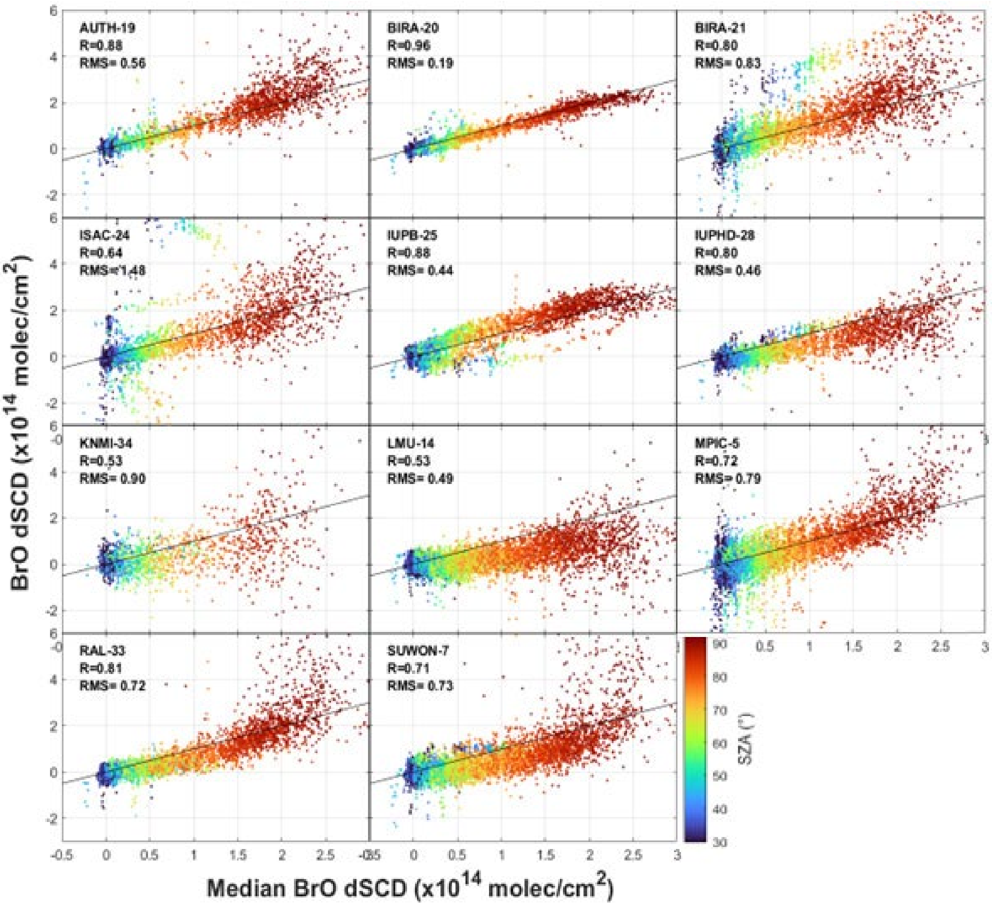

Figure 6: Same as Figure 3 but using centrally processed BrO dSCDs instead of individual datasets produced by participants.

In a second step, we modified the QDOAS configuration to incorporate the new retrieval settings covering the extended 336.5-359 nm wavelength interval. Results from the same analysis are displayed in Figure 6. The same medians have been used in Figures 3, 5 and 6 so a direct comparison can be made. As already observed for instrument #20 (Figure 5), the switch to the extended retrieval settings reduces substantially the noise of the comparisons for all instruments. The overall agreement with the median values derived from individual data processed in the standard (2-band) interval indicates that BrO dSCDs retrieved in both intervals are consistent with each other.

To further study the level of consistency between the two intervals, we have calculated (for each instrument) the median value of the BrO dSCDs between 80 and 90 degrees of solar zenith angle. This range of SZA is typically used for stratospheric BrO inversions. Results are shown in Figure 7(a) together with the medians of the dSCD standard errors (Figure 7(b)).

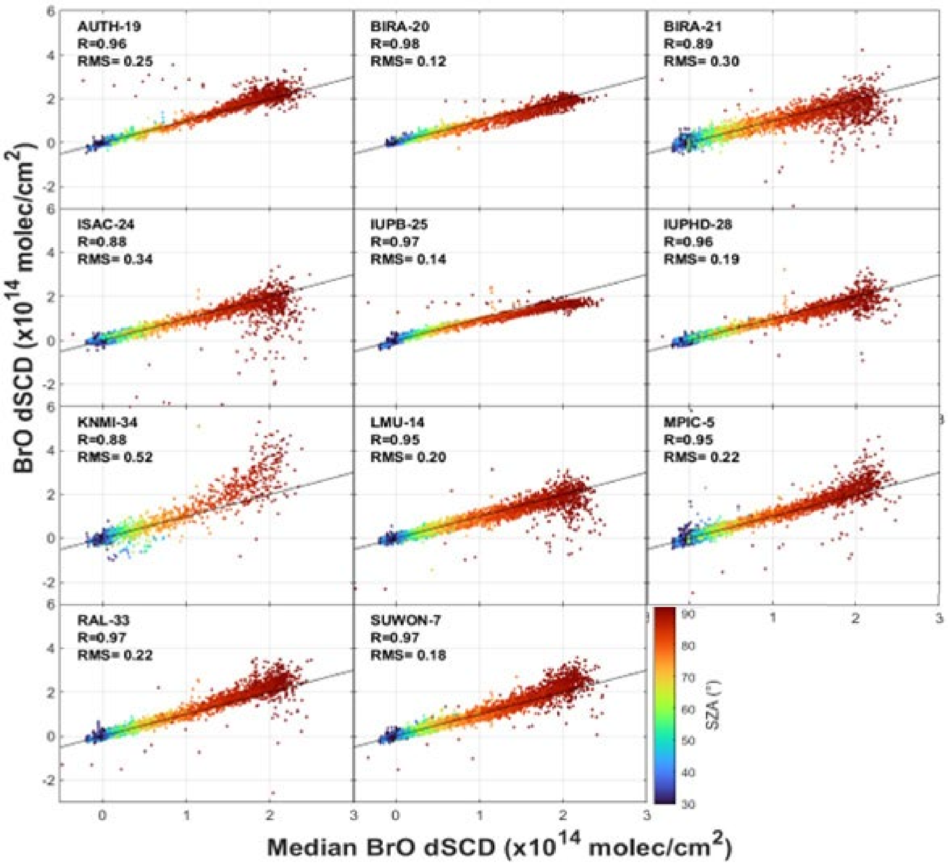

Figure 7: Same as Figure 5. In this configuration BrO dSCDs have been centrally processed using retrieval settings from Table 3.

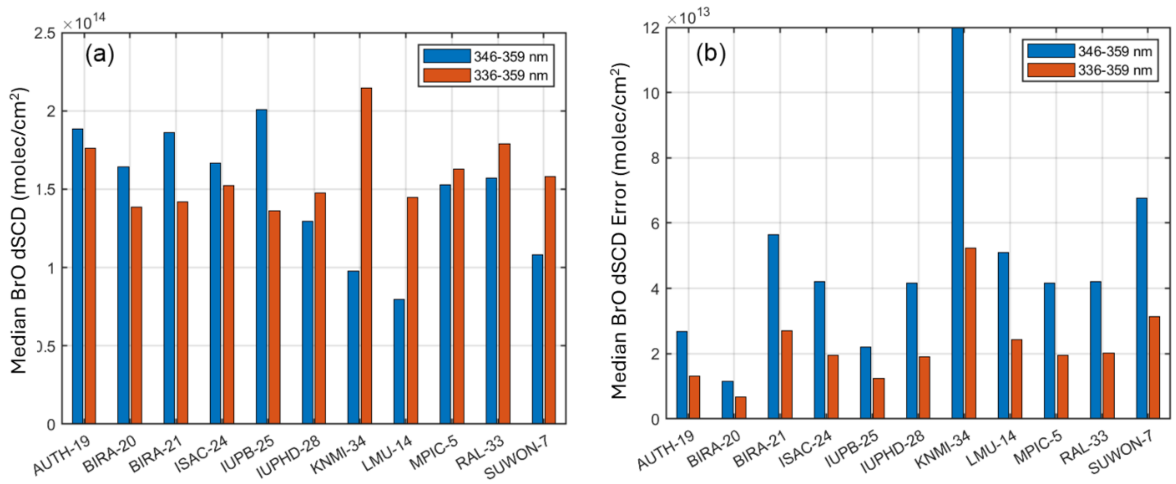

Figure 8: (a) Median of the BrO dSCDs retrieved, for each instrument, between 80 and 80° SZA using standard and extended DOAS fit settings, and (b) median of the dSCD fit errors in the same range of SZA.

As can be seen, retrievals in the extended window produce more consistent results among instruments. The reduction of the noise already clear from Figure 6, also translates into reduced fitting uncertainties for all participating instruments. Figure 7(a) also allows comparison of the consistency of the BrO dSCDs retrieved in both fitting intervals. For about half of the instruments (including instrument #20), the extended interval produces slightly smaller BrO dSCDs by about 10-15%, while for others an opposite behavior is observed. More work is needed to fully assess the consistency of the retrievals in both windows. Such an investigation would benefit from an extension of the study to more instruments/site, which is the subject of the next section.

5. Additional retrievals using station data

To complement the analysis based on measurements performed during the CINDI-3 campaign, data from 7 UV-Vis monitoring stations were collected and processed using harmonized retrieval settings. For each site, one full month of data was processed using the QDOAS software. In addition to the fitting windows already tested with CINDI-3 data (exploiting and 4 absorption bands of BrO), and intermediate spectral range covering 3 BrO bands was included. Details on the settings applied for the 3 fitting windows are given in Table 5.

The motivation of this exercise is to assess whether conclusions drawn during the CINDI-3 campaign remain valid when extending the retrieval test to more widespread conditions, i.e. stations operated in different latitudinal bands (mid- and high latitudes) and for instruments of new and older designs.

Table 4: List of the stations involved in the BrO SCD retrieval exercise. One month of data was processed at each site.

Station	Lat, Long	Station PI	Data processed
Harestua	60°N, 10°E	M. Van Roozendael	March 2013
Jungfraujoch	46.5°N, 8°E	M. Van Roozendael	March 2024
Kiruna	67.9°N, 21°E	T. Wagner	March 2013
Lauder	45°S, 169.7°E	R. Querel	March 2017
Marambio	64.2°S, 56.6°W	M. Yela	January 2018
Neumayer	70.7°S, 8.3°E	U. Friess	March 2019
Ny Alesund	78.9°N, 11.9°E	A. Richter	March 2025

Table 5: Retrieval settings applied to station data. The source of the absorption cross-sections is the same as described in Tables 2 and 3.

Wavelength range	336.5-359.0 nm	341.0-359.0 nm	346.0-359 nm
Cross-sections:			
BrO (223 K)	X	X	X
NO_2 (220 K)	X	X	X
HCHO (298 K)	X	X	
O_3 (223 K)	X, with Pukite terms	X, with Pukite terms	X
O_3 (243 K)	X	X	X
O_4 (293 K)	X	X	X
OClO (213 K)	X	X	X
Ring (250 K)	X, with slope and O_3 correction	X, with slope and O_3 correction	X, with slope

Ring (220 K)	X	X	
Polynomial degree	Order 5	Order 5	Order 3
Intensity offset	Slope	Slope	Slope

Figure 9 shows typical examples of the BrO dSCD diurnal patterns observed at each station, in the 3 fitting windows. In all stations except NyAlesund, reference spectra were selected each day at the minimum solar zenith angle. For Ny Alesund, a fixed reference spectrum (selected on the last day of the month) was used for the whole month, which means that for this site the dSCDs are not expected to be equal to zero at noon on days other than 31/03/2025.

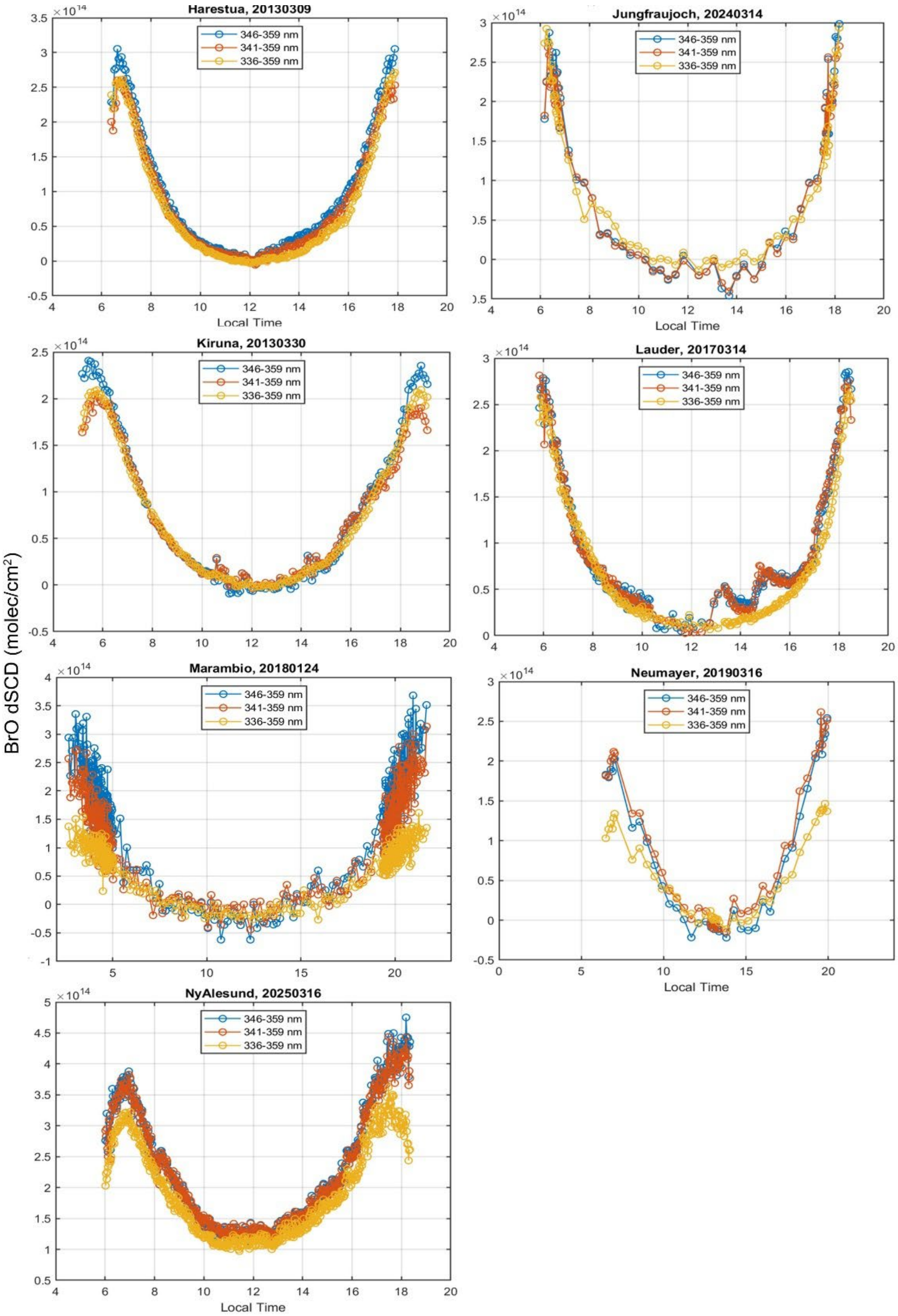

Figure 9: Example of BrO dSCD diurnal variations retrieved at the different test sites. Retrieval settings described in Table 5 were consistently applied to all instruments.

As can be seen, the ways the different instruments react to the different retrieval settings present similitudes but also large differences.

- The retrievals using 2 and 3 bands are in good overall agreement at all sites, although in Harestua and Kiruna, results using 3 bands (in red) tend to be smaller at the largest solar angles.
- Results using 4 bands (336.5-359 nm) tend to underestimate values in other intervals. In Neumayer and Marambio, the effect is more pronounced than in other sites. This behavior might be related to a residual ozone misfit, due to a lack of knowledge of the instrumental lineshape or other effects that may affect the accuracy of the ozone fit.
- Results using 4 bands are less noisy and more stable (less affected by artefacts) around noon at small SZA. This is particularly obvious in Lauder, but also clearly visible in other sites.

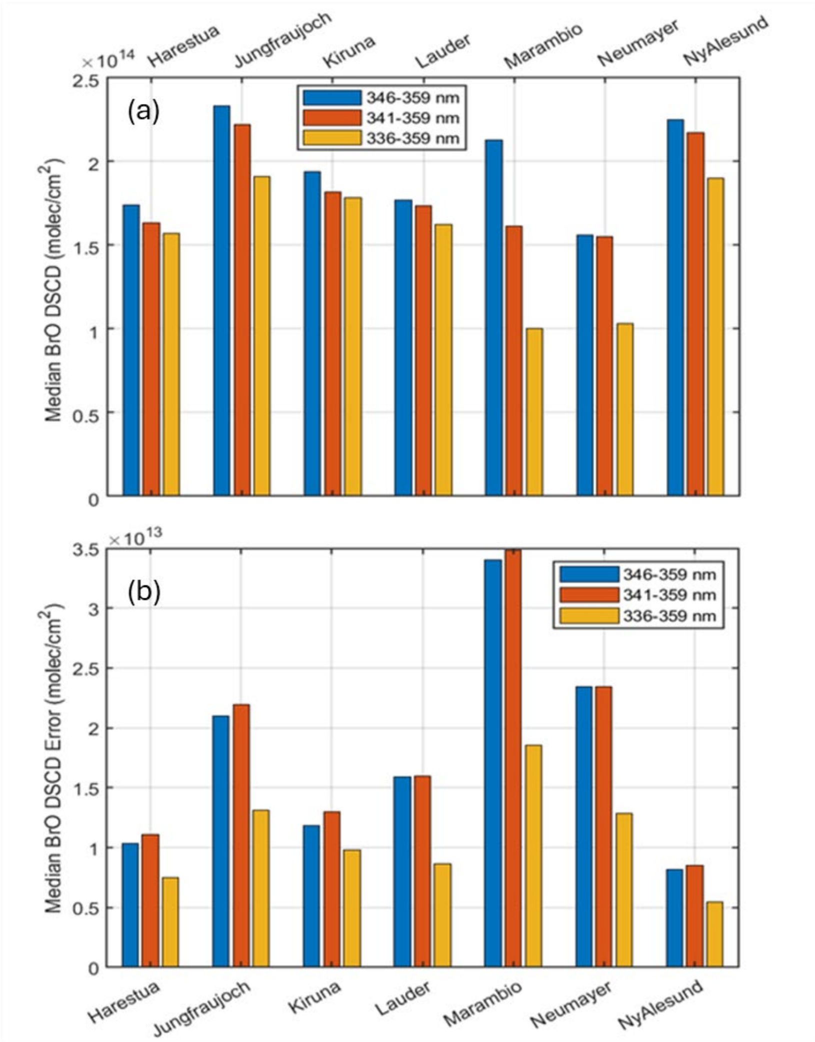

Figure 10: (a) Median of the BrO dSCDs retrieved between 80° and 90° SZA using 3 different retrieval windows; (b) median of the BrO dSCD fit errors in the same range of SZA.

To assess the impact of applying the 3 different settings in a more quantitative way, we have calculated the median BrO dSCDs from each instrument and each fitting window in a range of SZA going from 80 to 90°. Also, the median of the fitting error (one sigma) was calculated for the same selection of data. Results are displayed in Figure 10. In contrast to CINDI-3 data, the absolute values of the dSCDs cannot be compared here (since they correspond to different sites and different months). However, the consistency across the different fitting intervals can be evaluated. Main conclusions are as follows:

- The agreement between retrievals using 2 and 3 BrO bands is generally good or very good. The noise level is similar in both intervals, so there is no major gain moving from 2 to 3 bands. Similar conclusions can be derived from Figure 9.
- The BrO dSCDs retrieval in the large (4 bands) interval are less noisy than in other windows, but they tend to be underestimated, especially in Marambio and Neumayer. This behavior might be related to a larger ozone misfit, possibly due to a lack of proper knowledge of the instrumental lineshape of other instrument-related issues that may develop stronger at shorter wavelengths (e.g. straylight).
- The level of noise depends on the instrument specificities. Out of the 7 instruments tested here, the Ny Alesund system from IUP-UB provides the smallest fitting uncertainties.
- To better assess the expected level of consistency between the different fitting windows (excluding instrumental effects), additional test using synthetic data might be useful, and will be considered in a possible follow-up activity.

6. Analysis of long-term historical data series at Harestua (60°N) and Lauder (45°S)

Long-term UV-Vis measurements started in the nineties have been performed as part of the Network for the Detection of Atmospheric Composition Changes (NDACC) at the Harestua (60°N) and Lauder (45°S) stations. At both sites, major renovations requiring the replacement of spectrometers and detectors took place halfway through the time series (in 2012 at Harestua and in 2007 at Lauder). For these reasons, the datasets available in Harestua and Lauder are particularly well suited to test the stability of the BrO retrieval in time, as well as its sensitivity to important instrumental changes.

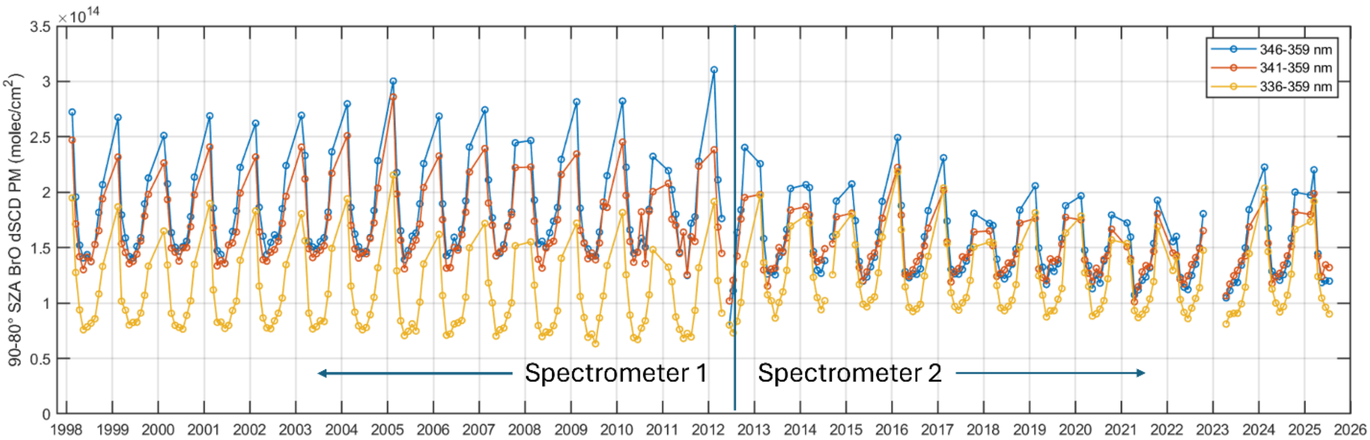

Figure 11: Time-series of monthly-averaged evening 90-80° SZA BrO dSCDs retrieved at Harestua, Norway (60°N) in the period from 1998 to 2025. Three different spectral fitting windows were used for the retrieval according to table 5. Different spectrometers were used during the two successive periods shown in the graph.

Following the same approach as in section 5, we conducted a full reprocessing of the spectral data available at both sites, using the 2-, 3- and 4-band retrieval settings described in Table 5. Results displayed in Figures 11 and 12 present monthly averages of the difference in BrO dSCDs between 90 and 80° SZA, for Harestua and Lauder respectively. In first good approximation, this quantity is proportional to the stratospheric BrO vertical column (see e.g. Sinnhuber et al., 2002).

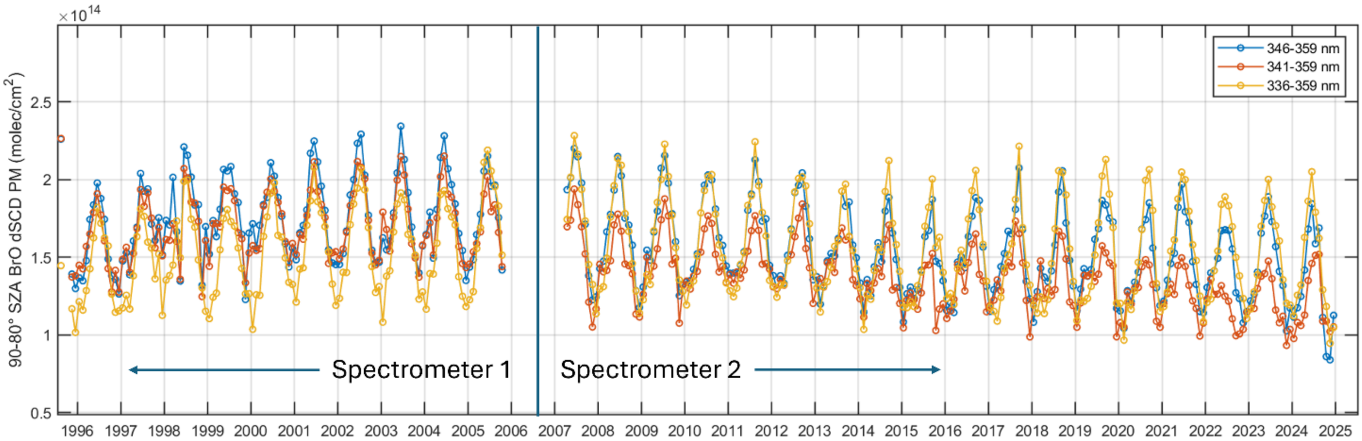

Figure 12: Time-series of monthly-averaged evening 90-80° SZA BrO dSCDs retrieved at Lauder, New-Zeeland (45°S) in the period from 1996 to 2024. As for Harestua, different spectrometers were used during the two successive periods shown in the graph.

For Harestua, we can conclude that the BrO dSCDs retrieved using 2 and 3 bands (in blue and red) are consistent with each other, especially during summer and spring. On the other hand, the 4-band retrieval reports lower dSCDs, with a different level of bias for the two spectrometers.

For Lauder, the situation is slightly different. There, we see a different behavior developing with the two successive spectrometers. In the first period, there is a good agreement between the retrievals using 2 and 3 bands while the 4-band analysis leads to a negative bias in comparison to other retrievals. This behavior is similar to the one observed in Harestua, although the amplitude of the observed bias is slightly smaller. During the second period, there is an excellent agreement between the 2- and 4-band analysis, while the 3-band retrieval appears to be biased low and somehow less stable in time. Overall (considering both spectrometers), the best consistency is achieved using the 2-band retrieval.

In Figure 13, we compare the consistency of the results at both stations. When selecting data sets showing the best overall stability at each site, i.e. using 3 bands at Harestua (341-359 nm) and 2 bands at Lauder (346-359 nm), we find that both data sets present a very good consistency in terms of the BrO dSCD levels as well as their seasonal variations and long-term trends. In particular, the known positive trend in the early years (until about 2001) followed by a negative trend due to the progressive release of inorganic bromine species from the stratosphere (Hendrick et al., 2008) is consistently captured at both sites.

Overall, the results obtained in Harestua and Lauder confirm the conclusions raised from the limited analysis performed in section 5. Although a significant gain in terms of fitting uncertainty can be obtained by extending the BrO retrieval to 4 absorption bands, the stability of the resulting BrO dSCDs can be compromised (at least for retrievals at large SZAs) in a manner that seems to depend on instrumental characteristics.

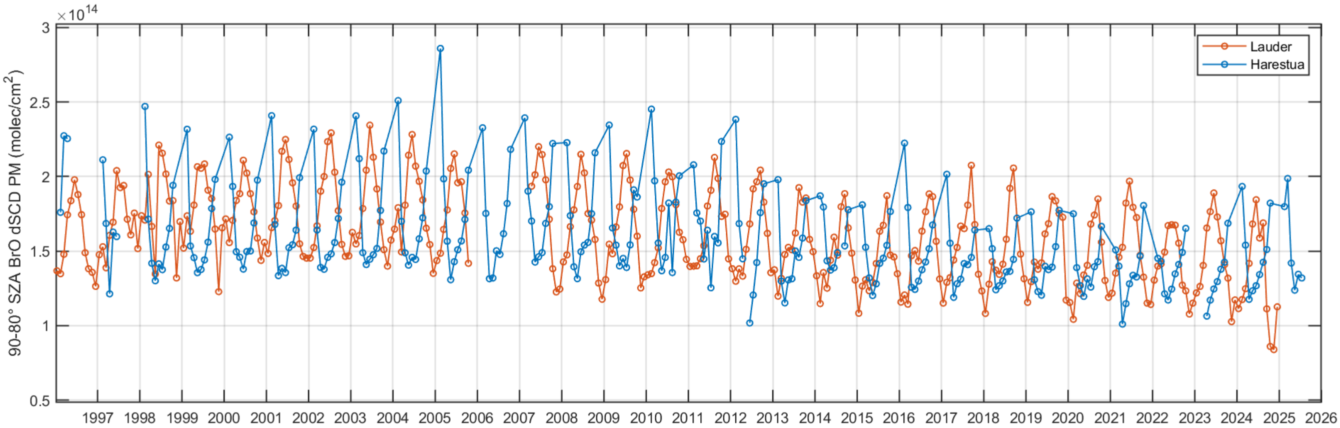

Figure 13: Comparison of BrO dSCDs retrieved in Harestua (341-359 nm) and Lauder (346-359 nm) from 1996 until 2025, for evening conditions. Both data sets show consistent seasonal variations as well as long-term variations.

7. Conclusions

The CINDI-3 campaign provided a useful set of measurements for studying the BrO retrieval from a wide range of instruments having different technical specifications and performance levels. The analysis of BrO dSCDs provided by individual participants using standardized settings imposed for the campaign reveals a large scatter overall, with significant differences depending on instrument specifications. Further evaluations using newly proposed retrieval settings covering a larger spectral range including up to 4 bands of BrO absorption (rather than 2 for standard settings) show promising results with a stabilization of the retrievals and a significant reduction of the BrO fitting uncertainty.

Using L1 data provided by participants in a standardized netCDF format, we expanded the analysis by centrally processing data from 11 instruments of different types (research-grade, Airyx SkySpec, and Pandora). Results confirm the benefits of the new retrieval settings. In all cases, we observe a systematic reduction of the noise, while median BrO dSCDs values remain consistent in both intervals.

These results suggest that the extended retrieval settings might provide a good baseline for central processing of BrO data within the FRM4DOAS system and could allow the integration of a large variety of instrumental configurations.

In order to further evaluate the applicability of these new settings, additional tests were conducted using data from existing NDACC stations. L1 data from 7 sites were included in this analysis that covered one month data at each station. They were processed using a standardized QDOAS configuration consistently applied to all instruments. In each case, three different fitting intervals were evaluated, covering respectively 2, 3 and 4 bands of BrO absorption. Results indicate that consistent BrO dSCDs can be obtained using 2 or 3 bands, but that the 4-band analysis tends to produce a negative bias at some stations.

In a last step, the analysis was extended to the processing of long-term observations covering several decades at the stations of Harestua (60°N) and Lauder (45°S). The results confirm that stable results covering a long period of time, also involving instrumental changes, cannot be easily obtained with the 4-band retrieval baseline. Optimal retrieval settings might have to be assessed individually for each instrument and might also depend on the focus of the measurements.

In summary, the 2 band-settings are more noisy but more stable and less prone to instrument-specific sources of bias. However, for FRM4DOAS, we recommend to test stability of instruments w.r.t different retrieval settings as part of the integration process.

8. References

Hendrick, F., Van Roozendael, M., Chipperfield, M. P., Dorf, M., Goutail, F., Yang, X., Fayt, C., Hermans, C., Pfeilsticker, K., Pommereau, J.-P., Pyle, J. A., Theys, N., and De Mazière, M.: Retrieval of stratospheric and tropospheric BrO profiles and columns using ground-based zenith-sky DOAS observations at Harestua, 60° N, Atmos. Chem. Phys., 7, 4869–4885, https://doi.org/10.5194/acp-7-4869-2007, 2007.

Hendrick, F., Johnston, P. V., De Mazière, M., Fayt, C., Hermans, C., Kreher, K., Theys, N., Thomas, A., & Van Roozendael, M., One-decade trend analysis of stratospheric BrO over Harestua (60°N) and Lauder (45°S) reveals a decline. Geophysical Research Letters, 35(14), 1–5. https://doi.org/10.1029/2008GL034154, 2008.

Aliwell, S. R., Van Roozendael, M., Johnston, P. V, Richter, A., Wagner, T., Arlander, D. W., Burrows, J. P., Fish, D. J., Jones, R. L., Tørnkvist, K. K., Lambert, J., Pfeilsticker, K., & Pundt, I., 2002, Analysis for BrO in zenith-sky spectra : An intercomparison exercise for analysis improvement. *J. Geophys. Res.*, *107*, 1–20. https://doi.org/10.1029/2001JD000329, 2002.

Chance, K. V, and R. J. D Spurr, Ring effect studies: Rayleigh scattering, including molecular parameters for rotational Raman scattering, and the Fraunhofer spectrum. Applied Optics, 36(21), 5224–5230, 2000. http://www.ncbi.nlm.nih.gov/pubmed/18259337

Chance, K., and R.L. Kurucz, An improved high-resolution solar reference spectrum for earth's atmosphere measurements in the ultraviolet, visible, and near infrared. Journal of Quantitative Spectroscopy and Radiative Transfer, 111(9), 1289–1295, https://doi.org/https://doi.org/10.1016/j.jqsrt.2010.01.036, 2010.

Finkenzeller, H., & Volkamer, R., O2–O2 CIA in the gas phase: Cross-section of weak bands, and continuum absorption between 297–500 nm. Journal of Quantitative Spectroscopy and Radiative Transfer, 279, 108063. https://doi.org/https://doi.org/10.1016/j.jqsrt.2021.108063, 2022.

Fleischmann, O. C., Hartmann, M., Burrows, J. P., & Orphal, J., New ultraviolet absorption cross-sections of BrO at atmospheric temperatures measured by time-windowing Fourier transform spectroscopy. Journal of Photochemistry and Photobiology A: Chemistry, 168(1–2), 117–132. https://doi.org/http://dx.doi.org/10.1016/j.jphotochem.2004.03.026, 2004.

Meller, R. and G.K. Moortgat, Temperature dependence of the absorption cross sections of formaldehyde between 223 and 323 K in the wavelength range 225-375 nm, J. Geophys. Res. D 105, 7089-7101, 2000.

Puķīte, J., Kühl, S., Deutschmann, T., Platt, U., and Wagner, T.: Extending differential optical absorption spectroscopy for limb measurements in the UV, Atmos. Meas. Tech., 3, 631–653, https://doi.org/10.5194/amt-3-631-2010, 2010.

Rothman, L. S., Gordon, I. E., Babikov, Y., Barbe, A., Chris Benner, D., Bernath, P. F., Birk, M., Bizzocchi, L., Boudon, V., Brown, L. R., Campargue, A., Chance, K., Cohen, E. A., Coudert, L. H., Devi, V. M., Drouin, B. J., Fayt, A., Flaud, J. M., Gamache, R. R., Harrison, J. J., Hartmann, J. M., Hill, C., Hodges, J. T., Jacque- mart, D., Jolly, A., Lamouroux, J., Le Roy, R. J., Li, G., Long, D. A., Lyulin, O. M., Mackie, C. J., Massie, S. T., Mikhailenko, S., Müller, H. S. P., Naumenko, O. V., Nikitin, A. V., Orphal, J., Perevalov, V., Perrin, A., Polovtseva, E. R., Richard, C., Smith, M. A. H., Starikova, E., Sung, K., Tashkun, S., Tennyson, J., Toon, G. C., Tyuterev, V. G., and Wagner, G.: The HITRAN2012 molecular spectroscopic database, J. Quant. Spectrosc. Ra., 130, 4–50, https://doi.org/10.1016/j.jqsrt.2013.07.002, 2013.

Serdyuchenko, A., Gorshelev, V., Weber, M., Chehade, W., and Burrows, J. P.: High spectral resolution ozone absorption cross-sections – Part 2: Temperature dependence, Atmos. Meas. Tech., 7, 625–636, https://doi.org/10.5194/amt-7-625-2014, 2014.

Sinnhuber, B.-M., Arlander, D. W., Bovensmann, H., Burrows, J. P., Chipperfield, M. P., Enell, C.-F., Frieß, U., Hendrick, F., Johnston, P. V., Jones, R. L., Kreher, K., Mohamed-Tahrin, N., Muller, R., Pfeilsticker, K., Platt, U., Pommereau, J.-P., Pundt, I., Richter, A., South, A. M., … Wittrock, F., Comparison of measurements and model calculations of stratospheric bromine monoxide. *Journal of Geophysical Research*, *107*(D19), 4398. https://doi.org/10.1029/2001JD000940, 2002.

Thalman, R., and R. Volkamer, Temperature dependent absorption cross-sections of O2-O2 collision pairs between 340 and 630 nm and at atmospherically relevant pressure. Phys. Chem. Chem. Phys., 15(37), 15371–15381. https://doi.org/10.1039/C3CP50968K, 2013.

Vandaele, A.C., C. Hermans, P.C. Simon, M. Carleer, R. Colins, S. Fally, M.F. Mérienne, A. Jenouvrier, and B. Coquart, "Measurements of the NO2 absorption cross-sections from 42000 cm-1 to 10000 cm-1 (238-1000 nm) at 220 K and 294 K", J. Quant. Spectrosc. Radiat. Transfer 59, 171-184, DOI: 10.1016/S0022-4073(97)00168-4, 1998.

Vandaele, A.C. & Hermans, Christian & Fally, Sophie. (2009). Fourier transform measurements of SO2 absorption cross sections: II. Temperature dependence in the 29 000-44 000 cm-1 (227-345 nm) region. Journal of Quantitative Spectroscopy and Radiative Transfer. v110. 2115-2126. 10.1016/j.jqsrt.2009.05.006.

Wagner, T., Dix, B., Friedeburg, C. v., Frieß, U., Sanghavi, S., Sinreich, R., & Platt, U., MAX-DOAS O4 measurements - A new technique to derive information on atmospheric aerosols. (I) Principles and information content. J. Geophys. Res., 109(D22), D22205. https://doi.org/10.1029/2004JD004904, 2004.

Wagner, T., Beirle, S., and Deutschmann, T.: Three-dimensional simulation of the Ring effect in observations of scattered sun light using Monte Carlo radiative transfer models, Atmos. Meas. Tech., 2, 113–124, https://doi.org/10.5194/amt-2-113-2009, 2009.